NIH-PA Author Manuscript

NIH-PA Author Manuscript

NIH-PA Author Manuscript

Quantitative Techniques for Assessing and Controlling the Dispersion and Biological Effects of Multi-walled Carbon Nanotubes in Mammalian Tissue Culture Cells

Xiang Wang[†,‡,#], **Tian Xia**[†,‡,#], **Susana Addo Ntim**[§], **Zhaoxia Ji**[‡], **Saji George**[†,‡], **Huan Meng**[†,‡], **Haiyuan Zhang**[†,‡], **Vincent Castranova**[¶], **Somenath Mitra**[§], and **André E. Nel**[†,‡,*]

[†]Division of NanoMedicine, Department of Medicine, University of California, Los Angeles, CA 90095, USA

[‡]California NanoSystems Institute, University of California, Los Angeles, CA 90095, USA

[§]Department of Chemistry and Environmental Science, New Jersey Institute of Technology, Newark, NJ 07102, USA

[¶]NIOSH, 1095 Willowdale Road, Morgantown, West Virginia 26505, USA

Abstract

In vivo studies have demonstrated that the state of dispersion of carbon nanotubes (CNT) plays an important role in generating adverse pulmonary effects. However, little has been done to develop reproducible and quantifiable dispersion techniques to conduct mechanistic studies *in vitro*. This study was to evaluate the dispersion of multi-walled carbon nanotubes (MWCNT) in tissue culture media, with particular emphasis on understanding the forces that govern agglomeration and how to modify these forces. Quantitative techniques such as hydrophobicity index, suspension stability index, attachment efficiency and dynamic light scattering were used to assess the effects of agglomeration and dispersion of as-prepared (AP), purified (PD) or carboxylated (COOH) MWCNT on bronchial epithelial and fibroblast cell lines. We found that hydrophobicity is the major factor determining AP- and PD-MWCNT agglomeration in tissue culture media but that the ionic strength is the main factor determining COOH-MWCNT suspendability. Bovine serum albumin (BSA) was an effective dispersant for MWCNT, providing steric and electrosteric hindrance that are capable of overcoming hydrophobic attachment and the electrostatic screening of double layer formation in ionic media. Thus, BSA was capable of stabilizing all tube versions. Dipalmitoylphosphatidylcholine (DPPC) provided additional stability for AP-MWCNT in epithelial growth medium (BEGM). While dispersion state did not affect cytotoxicity, improved dispersion of AP- and PD-MWCNT increased TGF-β1 production in epithelial cells and fibroblast proliferation. In summary, we demonstrate how quantitative techniques can be used to assess the agglomeration state of MWCNT when conducting mechanistic studies on the effects of dispersion on tissue culture cells.

Keywords

[*]Corresponding Author: André E. Nel, M.D./Ph.D., Department of Medicine, Division of NanoMedicine, UCLA School of Medicine, 52-175 CHS, 10833 Le Conte Ave, Los Angeles, CA 90095-1680. Tel: (310) 825-6620, Fax: (310) 206-8107, anel@mednet.ucla.edu.
[#]Contributed equally to this work.

Introduction

Carbon nanotubes (CNT) were first described in 1991. [1] This type of carbon allotrope exhibits a high surface area, high mechanical strength, ultra-light weight, enhanced electrical conductivity, and excellent chemical as well as thermal stability. [2] Because of these novel properties CNT are being used for a wide range of applications such as electronics, field emission devices, energy storage devices, sensors and drug delivery devices. [3, 4] However, in spite of their obvious commercial value, the safety of these materials needs to be considered in occupational, consumer and environmental settings. At least two important toxicological scenarios have emerged that raise safety concerns, namely the ability of multi-walled and single-walled CNT to generate granulomatous inflammation or fibrotic responses in the lung as well as mesothelial inflammation in rodents. [5–10] While similar pathology or disease processes have not been described for MWCNT in humans, the animal studies point to the importance of establishing screening procedures to assess CNT safety as well as avoidance of inhalation exposures in the workplace. [11]

In order to plan and conduct reproducible biological experiments, it is important to evaluate the physicochemical characteristics that influence CNT bioavailability and interactions at the nano-bio interface. One of the key physicochemical characteristics that determine biological responses in the rodent lung is the state of CNT dispersion, with agglomerated CNT more prone to be deposited in proximal airway where they induce granulomatous inflammation as compared to better dispersed tubes that are capable of deposition in alveoli and interstitial spaces, where they elicit interstitial fibrosis. [12] It is important, therefore, to understand the effects of the biological media on the characteristics of CNT, particularly their state of suspension and how that influences bioavailability and biological outcome. It is also important to understand how to control the state of CNT agglomeration under biological conditions to compare the clumped with the better dispersed tubes. Some of the key factors involved in CNT agglomeration are hydrophobicity, attractive van der Waals forces and the potential influence of electrical double layer formation on the surface of functionalized CNT. [13] While it is known that CNT can be transiently de-agglomerated by mechanical methods such as vortexing and sonication, appropriate dispersants are needed to stabilize the tube suspensions through provision of steric hindrance, electrostatic or electrosteric effects. Although effective dispersants such as N, N-dimethylformamide (DMF), N-methylpyrrolidone (NMP) [14, 15] or natural organic matter (NOM) [16–18] have been identified, these are not appropriate for studying CNT effects under tissue culture conditions. However, a number of proteins and non-toxic surfactants have emerged that could be applied to control the state of tube dispersion in biological conditions. For example, fetal bovine serum (FBS) is a useful dispersant in tissue culture media, [19, 20] while *in vivo* studies have identified the effectiveness of 1% Tween 80 as a dispersant in phosphate buffered saline (PBS). [6, 8] In addition, Dr. Castranova and colleagues have reported the use of lung lining fluid obtained by bronchoalveolar lavage (BAL) of rodents as an effective dispersing medium for carbon-based nanoparticles. [21] The same group also formulated an artificial lung lining fluid that can be reconstituted through mixing of serum albumin with the phospholipid surfactant, dipalmitoyl phosphatidylcholine (DPPC).[22] Indeed, independent studies have confirmed the synergistic effects of proteins and surfactants in CNT dispersion. [23, 24] Finally, it is important to point out that most of the aforementioned studies have been executed on single or a limited number of tube formulations that did not include a systematic variation in CNT physicochemical properties to compare dispersants that are specifically chosen to modify tube behavior in buffered ionic conditions.

In this study, we used purified (PD) and carboxyl-functionalized (COOH) derivatives of as-prepared MWCNT (AP) to develop quantitative methods for assessing the suspension of these tubes in water and tissue culture media, including the use of these methods to select for

the optimal dispersion to perform mechanistic cell culture studies. We demonstrate the practical use of a partitioning coefficient, suspension stability index, attachment efficiency, and dynamic light scattering (DLS) in a systematic approach to stabilization of MWCNT suspension through the use of BSA and DPPC. We demonstrate that BSA and DPPC function in additive fashion to disperse hydrophobic AP-MWCNT in an epithelial growth medium and that this leads to increased TGF-β1 production in a bronchial epithelial cell line. Moreover, better-dispersed MWCNT also increased fibroblast proliferation, in agreement with similar observations in the rodent lung. [7, 12] Quantifiable methods to determine the state of CNT dispersal will be of great benefit in executing biological experiments on these materials.

Results and Discussion

Characterization of MWCNT

The original supply of AP-MWCNT from Cheap Tubes Inc. served as the stock for preparing purified (PD) and carboxylated (COOH) derivatives. This derivatization provided a small library of materials that could be systematically compared for the influence of hydrophobicity, hydrophilicity and electrical double layer formation on tube agglomeration in biological media and the resultant effect on the cell biological responses. The baseline physicochemical characteristics of the materials are listed in Table 1. While AP-MWCNT contained ~5.25 wt. % metal impurities, purification decreased this to ~1.88 wt. %. Further acid treatment of the PD-MWCNT introduced carboxyl groups on 5.27 % of the carbon backbone (on a per weight basis). The carboxyl functionalization considerably increased the negative surface charge on the tubes, which makes them more hydrophilic but at the same time lays the platform for electrical double layer formation that could affect COOH-MWCNT dispersion according to the tenets of Derjaguin, Landau, Verwey and Overbeek (DLVO) theory. [25] The structure of the MWCNT was further analyzed by SEM and FTIR spectroscopy as demonstrated in Fig. 1. The SEM images show that acid treatment did not cause structural damage, allowing the tubes to remain intact (Fig. 1A). FTIR spectroscopy confirmed the carboxyl functionalization (Fig. 1B).

Assessment of the Contribution of Hydrophobicity in AP- and PD-MWCNT Agglomeration and Preventing This Attachment by Steric and Electrosteric Hindrance

We used *n*-octanol/water partitioning to establish a hydrophobicity index for the different MWCNT derivatives (Fig. 2). This index was calculated using the light absorbance of AP-MWCNT, PD-MWCNT and COOH-MWCNT at 550 nm wavelength in water or other aqueous media prior to as well as following *n*-octanol introduction as demonstrated in Fig. 2A. Fig. 2B compares the relative hydrophobicity indices of the tubes in distilled H_2O, phenol red-free Dulbecco's Modified Eagle's Medium (DMEM) and Bronchial Epithelial Basal Medium (BEBM). DMEM is a widely used tissue culture medium while BEBM is used for culturing bronchial epithelial cells. [26][27] The results show that while AP- and PD-MWCNT had relatively high hydrophobicity indices, favoring partitioning in the *n*-octanol phase, COOH-MWCNT was more hydrophilic and favored partitioning in the aqueous phase (Fig. 2B). Visual inspection of the phases confirmed that while AP-MWCNT and PD-MWCNT were located in the *n*-octanol layer or close to the interface (arrows), COOH-MWCNTs were homogeneously dispersed in the water or tissue culture media (Fig. S1, upper panel). The hydrophilicity of the carboxylated tubes agrees with their relatively high negative surface charge (zeta-potential of −50.30 mV) in water (Table 2), which provides electrostatic repulsion. In contrast, AP-MWCNT and PD-MWCNT exhibited slightly negative zeta-potentials of −14.5 and −8.73 mV, respectively. Please notice that although the experiment in Fig. 2 was conducted at a MWCNT concentration of 50 μg/mL, similar trends were obtained for with either lower (25 μg/mL) or higher (100 μg/mL) concentrations (not

shown). All considered, the relatively high hydrophobicity of AP-MWCNT and PD-MWCNT is a major factor contributing to their attachment in aqueous environments, while the electrostatic repulsion by their carboxyl groups promotes COOH-MWCNT hydrophilicity.

In order to limit the extent of MWCNT agglomeration for performing pulmonary exposure studies, it has been demonstrated by simple visual inspection approaches that the dispersion of single walled carbon nanotubes (SWCNT) and MWCNT can be improved by a surrogate lung lining fluid that is composed of serum albumin mixed with a surfactant, DPPC. [22] When BSA was introduced to the aqueous AP-MWCNT and PD-MWCNT suspensions during sonication, it could immediately be ascertained following *n*-octanol introduction that the tubes prefer the aqueous environment (water or tissue culture medium) in which they remain stably suspended (Fig. S1, lower panel). Interestingly, the addition of BSA changed the zeta-potentials of AP-MWCNT and PD-MWCNT from −14.50 to −28.61 mV and −8.73 to −31.76 mV (Table 2), respectively. This is due to direct BSA binding to the hydrophobic tube surfaces. [28] Once attached to the tube surfaces by sonication, flexible macromolecules such as BSA (hydrodynamic radius of ~7.5 nm by DLS) are capable of providing steric hindrance. [28] In addition, because of BSA's isoelectric point of ~4.7, this protein becomes anionic at pH   7, which explains the increased negative zeta-potential. This effect could contribute to electrosteric hindrance. Therefore, the major effect of BSA in stabilizing hydrophobic AP- and PD-MWCNT in water is through steric hindrance as well as electrosteric repulsion. By contrast, the major BSA influence on the hydrophilic COOH-MWCNT is a steric hindrance effect. While it is known that a number of proteins (*e.g.*, serum albumin, immunoglobulin, streptavidin) are capable of non-specific binding to CNT surfaces, [29] no previous effort has been made to quantify the degree of dispersal.

The Effect of Ionic Strength on Tube Agglomeration in Physiological Media

While ionic strength has no independent discernible effect on AP- and PD-MWCNT agglomeration (Fig. S2), the aqueous dispersion of COOH-MWCNT is clearly influenced by the addition of ionic charge, as demonstrated by the progressive decline of the suspension stability index with incremental concentrations of PBS (Fig. 3A). The addition of 0.9 % saline (Fig. 3C) or salt-containing biological media (Fig. S3) had similar destabilizing effects. According to the DLVO theory, the stability of a colloidal suspension is based on the net balance of two predominant forces, namely electrostatic repulsion that prevents and attractive van der Waals forces that promote agglomeration. [25] While in distilled water or dilute electrolyte solutions, the high negative wall surface potential of COOH-MWCNT is capable of overwhelming the van der Waals attractions, the addition of ionic charge leads to double layer formation and electrostatic screening of the wall charge, allowing the van der Waals forces to dominate (Fig. S4A). This leads to an increase of the attachment efficiency that can be quantitatively assessed by calculation of the α-factor for COOH-MWCNT (Fig. 3B). This calculation is made by using a laser to obtain DLS observations to feed into an equation that calculates an inverse stability ratio as demonstrated in Materials and Methods. Incremental PBS concentrations lead to a progressive increase in α (Fig. 3B).

Because it is desirable to keep COOH-MWCNT dispersed in ionic solutions, it is noteworthy that stable tube dispersions (>48 hr) could be achieved by addition of BSA to the PBS suspension (Fig. 3A and 3C, lower panel). BSA is equally effective in DMEM, BEBM and BEGM (BEBM supplemented with essential growth factors) (Fig. S3). The improved dispersal of COOH-MWCNT is accompanied by decreased attachment efficiency in PBS (Fig. 3B) and an increase in the tubes' suspension stability index (Fig. 3A). While BSA binding to the carboxylated tubes may involve hydrophobic vacancies that are interspersed with the COOH groups, it is also possible that this protein could attach to the negatively

charged tube surfaces *via* a Ca^{2+} bridge (Fig. S4B). This could provide steric and electrosteric hindrance that overcomes the reduced electrostatic repulsion as a result of electrical double layer formation on the COOH-MWCNTs surface (Fig. S4A).

The Use of BSA and DPPC to Stabilize MWCNT Dispersion in Tissue Culture Media for Cellular Studies

Since BSA interacts with hydrophobic (AP, PD) as well as carboxylated MWCNT to stabilize aqueous dispersions (Fig. 3C and Fig. S3), we made use of the versatile properties of this protein to implement quantative and reproducible methods for MWCNT dispersal to perform tissue culture experiments. The effect of BSA was studied in parallel with DPPC use to compare the protein's effect to that of the phospholipid detergent. [21, 23] To provide a quantitative assessment of the suspension stability index, we used UV-vis spectroscopy to assess time-dependent MWCNT sedimentation in the absence and presence of BSA and/or DPPC. The hierarchical order of the suspension stability index in BEGM was COOH-MWCNT > PD-MWCNT > AP-MWCNT (Fig. 4A). While DPPC coating did not improve the tendency to agglomerate, the addition of BSA significantly improved the stability index of PD-MWCNT and AP-MWCNT over a 20 hr observation period (Fig. 4A). Interestingly, while co-administration of DPPC significantly enhanced the ability of BSA to disperse the more hydrophobic AP-MWCNT, this detergent had no added effects on PD- and COOH-MWCNT dispersal (Fig. 4A). In order to determine whether the DPPC effect on AP-MWCNT is additive to BSA, we also estimated the stability index using equimolar quantities of DPPC, BSA and BSA+DPPC. This demonstrated that the combination of BSA and DPPC provided more stable dispersions than equimolar quantities of the individual dispersants (Fig. 4B). BSA and DPPC were equally effective at dispersing tubes at lower (25 µg/mL) and higher (100 µg/mL) as demonstrated in Fig. S5. Thus, the combination of BSA and DPPC provides an additive effect for the more hydrophobic AP-MWCNT. Whether this is due to random co-localization of the dispersants on the tube surface or a cooperative effect requires further study (Fig. S4C). Cooperative binding could involve interaction of the phospholipid fatty acid tails with the hydrophobic binding pockets that are being used for fatty acid transport. Thus, it is possible that cooperative binding on the tube surface could lead to a 3-way interaction between the tubes, BSA and DPPC.

Similar results were obtained when adding BSA to the epithelial growth medium, DMEM, except that the protein alone provided efficient dispersal of all tube formulations in the absence of DPPC (Fig. 5). The observation that DPPC was not required as an additional dispersant in BEGM could be due to the addition of bovine pituitary growth factors to this culture medium to promote epithelial cell growth. The extract contains a number of biomolecules such as lipids, peptides, and proteins that could contribute to tube dispersal. Interestingly, the agglomeration rates for each of the tube formulations were slower in DMEM than in BEGM (compare Fig. 4A with Fig. 5). Because the former medium is often used with FBS supplementation to yield complete DMEM (cDMEM), we also assessed the stability index in cDMEM. Even though cDMEM contains BSA, it was not quite as effective for tube dispersal as BSA alone (Fig. 5).

Based on the aforementioned findings, a mechanism for MWCNT de-agglomeration can be proposed where tube sonication in the presence of dispersing agents can be used to obtain stable suspensions in tissue culture media. Sonication provides a local shear force that opens up spaces at the end of the tube bundles or stacks. Once formed, these spaces become occupied by protein or detergent-like dispersants that lead to smaller and more stable tube agglomerates. [30] BSA is an effective dispersant that provides steric as well as electrosteric hindrance. When dealing with tubes that have a highly hydrophobic surface (*e.g.*, the AP-MWCNT in this study), DPPC may provide additional stabilization of the BSA effect (Fig.

4B). The implementation of quantitative methods for assessing tube stability in aqueous and ionic environments is a considerable improvement over more subjective techniques such as the use of light optical microscopy to visualize the agglomerate size. Nonetheless, the visual inspection confirms that BSA indeed leads to the forming of smaller tube stacks and that this effect is enhanced by DPPC when the more hydrophobic tubes are used in BEGM (data not shown). Although mathematically inaccurate for estimating the exact stack sizes, we could confirm that DLS is helpful for determining the relative hydrodynamic size of the tube agglomerates and can help to provide a semi-quantitative estimation of BSA and/or DPPC dispersing effects in tissue culture media (Fig. S6A and Fig. S6B).

The Dispersion State of MWCNT Affects Bronchial Epithelial and fibroblast responses

Previous studies reported that intratracheal instillation of poorly-dispersed SWCNT (large agglomerates, ~1.5 μm diameter) results in tube deposition in the terminal bronchioles and proximal alveoli, where the tubes elicit granulomatous inflammation. [8, 9] In contrast, well-dispersed SWCNT with a mean aggregate diameter of ~0.7 μm gain rapid access to the alveolar interstitial space where they induce a progressive fibrosis with minimal evidence of lung inflammation. [7, 12] A key question becomes whether the dispersion state of MWCNT affects cellular behavior, including biological responses that may be informative of pulmonary injury. In order to study the effects of tube dispersal states in a bronchial epithelial cell line, BEAS-2B, we first compared the tubes' influence on cell viability, LDH release and the production of TGF-β1, a fibroblast growth factor (Figs. 6 and S7). While neither agglomerated nor dispersed tubes had any effect on cellular metabolic activity (MTS assay, Fig. S7A) or LDH release (Fig. S7B), BEAS-2B cells did significantly increase TGF-β1 in production in response to well dispersed (BSA+DPPC) AP-MWCNT and PD-MWCNT (Fig. 6). In contrast, agglomerated tubes that were not treated with a dispersant (ND) had no effect on TGF-β1 production (Fig. 6). While small quantities of TGF-β1 were released from cells treated with COOH-MWCNT, the addition of dispersants had no effect (Fig. 6). In order to determine the relevance of TGF-β1 production on fibroblast growth potential, we also developed a proliferation assay using the human lung fibroblast cell line, CRL-1490. In this assay, the number of proliferating cells incorporating the fluorescent dye, EdU, is quantitatively expressed as a percentage of the total cell number (Hoechst nuclear staining) (Fig. S8A). Because transfer of the BEAS-2B supernatants interfered in CRL-1490 proliferation, we asked whether the exact amount of recombinant TGF-β1 (5–10 pg/mL) present in the BEAS-2B supernatant could induce CRL-1490 proliferation. Addition of 1.9–125 pg/mL TGF-β1 to the fibroblast culture medium increased the % EdU-positive cells in our fibroblast assay (Fig. S8B). Moreover, direct addition of dispersed (D) versus non-dispersed (ND) MWCNT to the fibroblast culture medium (Earl's Minimum Essential Medium, supplemented with 10 % FBS) elicited fibroblast proliferation in the presence of dispersed AP and PD tubes, while ND tubes had no effect (Fig. 7). In addition, dispersed COOH-MWCNT did not significantly increase fibroblast proliferation (Fig. 7).

While it is clear that in the dispersed state there is a definitive increase in the cellular response with increased dose of AP- or PD-MWCNT (Fig. 6), it is important to make the point that dispersal could affect the bio-available dose at the cellular level. While we do not understand as yet whether this translates into more tubes making contact with the cell membrane or more tubes being taken up into the cell, it is conceivable that both processes could be enhanced by better tube dispersal. In that case, improved tube dispersal could play a role in the local dosimetry that determines response outcome, either through cell membrane contact or intracellular uptake.

Hydrophobicity is a major factor that determines the dispersion state of AP-MWCNT and PD-MWCNT in water and cellular growth media. In contrast, the ionic strength of the solution is a major factor that influences the state of COOH-MWCNT agglomeration in

buffered salt-containing media. In spite of these different forces contributing to the agglomeration of different tube versions, BSA is an effective dispersant that de-agglomerates the tubes through a direct binding to the tube surfaces, using either hydrophobic or electrostatic binding interactions. BSA surface binding results in steric and electrosteric hindrance that is capable of stabilizing the MWCNT in suspension. While BSA is quite effective for MWCNT dispersion in different media, DPPC provides additional stability for more hydrophobic MWCNT in epithelial growth medium. Being able to perform quantitative assessment of the state of CNT dispersion or agglomeration in biological media is of importance for conducting mechanistic cellular studies that could inform us about adverse CNT effects in the lung. In this regard, we demonstrate that the dispersal state of AP- and PD-MWCNT impacts TGF-β1 production and fibroblast proliferation, which could explain why better dispersed tubes are more potent than non-dispersed tubes in inducing pulmonary fibrosis. [7] Our future studies will develop a predictive toxicological model based on these concepts. Being able to do high throughput comparison of CNT in tissue culture cells can help to gather data in large CNT batches for subsequent use to perform *in vivo* studies.

In addition to its effect on the physicochemical state of MWCNT dispersion, it is important to consider that BSA coating of the tubes' surfaces could have an independent influence on biological outcomes from the perspective of either promoting cellular contact or uptake or preventing cellular contact or uptake due to steric hindrance effect. While these concepts have been more comprehensively studied with respect to engineered nanoparticles, less is known about this topic for CNT and several fundamental issues need to be addressed regarding contact of the CNT with the cell membrane and possible intracellular uptake. [32, 33] Kam *et al.* have suggested that SWCNT are capable of traversing the cell membrane through endocytosis, whereas Pantarotto *et al.* have suggested that CNT could be translocated into the cell through a process that involves insertion and diffusion through the lipid bilayer. [34, 35] Moreover, Kam *et al.* have demonstrated that non-covalent conjugation of BSA or DNA to SWCNT surfaces lead to more avid tube uptake in HeLa and HL60 cells. Although we did not look at cellular uptake in this study, it is important to consider the possibility that in the generation of fibrogenic responses BSA could contribute to promoting cellular contact with the MWCNT. This would be equivalent to a scaffolding effect similar to the use of CNT in tissue engineering to promote the growth and proliferation of stem cells. While clearly more work is required in this area, it is important to point out that the BSA concentration (0.6 mg/ml or 0.06 %) we used in this study is very low and that from a pulmonary perspective this dose has been estimated to be 50 times less than undiluted alveolar lining fluid. [22] Moreover, Sager *et al*. and Porter *et al*. have shown that the experimental dose of BSA that we used do not alter the inflammatory potential of crystalline silica in rats or mice 1 day post-exposure. [21, 22] This suggests that BSA does not mask the bioactivity of these nanoparticles.

Materials and Methods

Carbon Nanotubes and Chemicals

The MWCNT stock was purchased as a powder from Cheap Tubes Inc. (Brattleboro, VT, USA). The stock preparation is also referred to as as-prepared (AP) nanotubes. Bronchial epithelial growth medium (BEGM) was obtained from Lonza (Mapleton, IL, USA), which is supplemented with a number of growth factors including bovine pituitary extract (BPE), insulin, hydrocortisone, hEGF, epinephrine, triiodothyronine, transferrin, gentamicin/amphotericin-B and retinoic acid. Dulbecco's modified eagle's medium (DMEM) with high glucose and phosphate buffered saline (PBS) were purchased from Invitrogen (Carlsbad, CA, USA). Earl's Minimum Essential Medium (EMEM) was purchased from the American

Type Culture Collection (ATCC, Manassas, VA, USA). Low-endotoxin bovine serum albumin (BSA) and fetal bovine serum (FBS) were from Gemini Bio-Products (West Sacramento, CA, USA). Dipalmitoylphosphatidylcholine (DPPC) and *n*-octanol were purchased from Sigma-Aldrich (St. Louis, MO, USA). All MWCNT stock solutions were prepared using pure deionized water (DI H_2O) with resistivity >18 MΩ-cm.

Physicochemical Characterization of MWCNT

The purification and functionalization of the MWCNT were accomplished as previously described. [36–38] This activity was carried out in a Microwave Accelerated Reaction System CEM Mars (Matthews, NC, USA) fitted with internal temperature and pressure controls. The 100 mL reaction chamber was lined with Teflon PFA® with an operating range of 0~200 °C and 0~200 psi. The residual metals were removed *via* microwave induced reaction with 1N HNO_3 followed by a reaction with saturated ethylenediamine tetra-acetate in CH_3COOH. [39] The purified MWCNT (PD-MWCNT) were added to the reaction chamber together with 40 mL of a mixture of 1:1 70 % nitric acid and 97 % sulfuric acid. With the microwave power set to 95 % of the maximal possible 1600 watt output, the reaction was carried out for 20 min at a temperature of 140 °C. The suspension was filtered through a 10 μm PTFE membrane, washed with deionized water (DI H_2O) to a neutral pH and vacuum dried at 70 °C. This sample derivative was designated COOH-MWCNT. A variety of different analytical techniques were used to characterize the MWCNT, including Energy Dispersive X-ray Spectroscopy (EDS, Oxford Instrument, Oxfordshire, UK) to identify the elemental composition of the MWCNT. The Fourier Transform Infrared spectroscopy (FTIR) measurements were carried out in purified KBr pellets using a PerkinElmer Spectrum One instrument (Downers Grove, IL, USA). Thermogravimetric analyses (TGA) were performed using a Pyris 1 TGA (Perkin-Elmer Inc., Covina, CA, USA) from 30 °C to 900 °C under a flow of air at 10 mL/min and a heating rate of 10°C per min. Scanning Electron Microscopy (SEM) using a LEO 1530 VP SEM equipped with an energy-dispersive X-ray analyzer was used to study the morphology of the samples. Zeta-potential measurements of the MWCNT suspensions were performed using a ZetaSizer Nano-ZS Instrument (Malvern Instruments, Worcestershire WR, UK). The relative hydrodynamic radius of MWCNT suspended in H_2O was measured using high throughput dynamic light scattering (HT-DLS, Dynapro™ Plate Reader, Wyatt Technology, Santa Barbara, CA, USA).

Preparation of MWCNT Suspension in Media

AP-, PD- and COOH-MWCNT were provided as dry powders. The samples were weighed on an analytical balance in the fume hood and suspended in DI H_2O at a concentration of 5 mg/mL in 4 mL glass vials. These suspensions were sonicated for 15 min in a water sonicator bath (Branson, Danbury, CT, USA, Model 2510, 100 W output power; 42 kHz frequency) and used as the stock solution for further dispersion in cell culture media. A water bath rather than a sonication probe was used to deliver a cavitation force suitable for de-agglomeration but not so high as to prevent protein attachment or tube damage. [40–42] An appropriate amount of each stock solution was added to achieve the desired final concentration. The diluted tube suspensions were vortexed for 15 s (fixed-speed vortex, 02-215-360, Fisher Scientific, Pittsburgh, PA, USA), sonicated for 15 min, and then vortexed for another 15 s vortex to obtain tube suspensions of 50 μg/mL (unless otherwise specified). Where dispersing agents were used, these were added to the culture media before the addition of the tubes. The final concentrations of BSA and DPPC were 0.6 mg/mL and 0.01 mg/mL, respectively, unless otherwise stated.

Assessment of the Hydrophobicity Index of MWCNT in Physiological Media

Partitioning of MWCNT in an *n*-octanol/aqueous interface was used to calculate a hydrophobicity index. [43, 44] After MWCNT suspension in the various aqueous media at a range (25–100 µg/mL) of concentrations, the absorbance (A) of the tubes was measured at 550 nm by UV-vis spectrometry (SpectroMax M5e, Molecular Devices Corp., Sunnyvale, CA, USA) based on previous work. [45] This value was designated A_0. An identical volume of *n*-octanol was added to the aqueous tube suspension, the vials vortexed for 15 s and then incubated at room temperature for 30 min. At this point the A value of the aqueous layer was re-measured (A_1) and hydrophobicity index calculated as follows:

$$\text{Hydrophobicity index} = \left(\frac{A_0 - A_1}{A_0} \right) \times 100\%$$

Characterization of MWCNT Suspension Stability Index

A kinetic analysis of suspension stability was performed by monitoring the aqueous solution absorbance at 550 nm for different lengths of time, using UV-vis spectrometry (SpectroMax M5e, Molecular Devices Corp., Sunnyvale, CA, USA). Typically, 1 mL of the MWCNT suspension at 25–100 µg/mL was prepared with or without dispersing agents and absorbance readings were taken at 1 hr time intervals for 20 hr.

Attachment Efficiency of COOH-MWCNT

A 90° light scattering unit (Malvern Instruments Zetasizer Nano ZS90, Worcestershire WR, UK) equipped with a 4 mW He-Ne laser with a frequency output of 632.8 nm was used to perform the CNT aggregation experiments. Agglomeration data were collected on 1 mg/mL dispersions of COOH-MWCNT in PBS and PBS + 0.6 mg/mL BSA. The PBS concentrations ranged from 6 mM to 150 mM. The dynamic light scattering measurements were collected at 25 °C. The incident laser beam and the autocorrelation function were allowed to accumulate for > 10 s after a 120 min temperature equilibration. The measurements were performed for a period of time ranging from 150 s to 3 hr. The initial rate of change in the hydrodynamic radius (R_h), $\left(\frac{dR_h}{dt} \right)_{t \to 0}$ is proportional to kn_o where k is the initial aggregation rate constant and n_o is the initial concentration of the MWCNT. [46] The inverse stability ratio ɑ or attachment efficiency was obtained from the following equation:

$$\alpha = \frac{\left(\frac{dR_h}{dt} \right)_{t \to 0}}{\left(\frac{dR_h}{dt} \right)_{(f)t \to 0}}$$

where $\left(\frac{dR_h}{dt} \right)_{(f)t \to 0}$ represents the fast aggregation regime. [18, 47, 48]

BEAS-2B Cellular Culture and Co-incubation with MWCNT

BEAS-2B cells were purchased from ATCC (Manassas, VA, USA) and cultured in a 5% CO_2 at 37 °C in BEGM in collagen-coated 75 cm^2 flasks. For exposure to MWCNT, aliquots of 1×10^4 cells were cultured in 0.2 mL medium in 96-well plates (Costar, Corning, NY, USA) at 37 °C for the indicated time periods. All the MWCNT solutions were freshly prepared. While non-dispersed (ND) MWCNT were vortexed for 15 s but not sonicated in BEGM that also contained no dispersants (BSA, DPPC or FBS), better dispersed (D)

MWCNT were prepared by sonication in BEGM containing BSA (at 0.6 mg/mL), DPPC (at 0.01 mg/mL) or a combination of both dispersants before being added to the tissue culture dishes.

ELISA for TGF-β1 Quantification

The TGF-β1 concentration in the BEAS-2B culture medium was determined by an $E_{max}^{®}$ ImmunoAssay System (Promega, Madison, WI, USA) according to the manufacturer's instructions. A 96-well plate was coated with monoclonal anti-TGF-β1 and the captured growth factor detected by polyclonal anti-TGF-β1 conjugated to horseradish peroxidase. Absorbance was measured at 450 nm using a plate reader (SpectroMax M5e, Molecular Devices Corp., Sunnyvale, CA, USA). Results were expressed as pg per mL.

Assessment of Fibroblast Proliferation using the EdU-based Proliferation Assay

The human lung fibroblast cell line, CRL1490, was obtained from the American Type Culture Collection (Manassas, VA, USA). The cells were cultured in EMEM supplemented with 10 % FBS, 100 U/mL penicillin and 100 μg/mL streptomycin. Cultures were maintained in a 5 % CO_2 humidified atmosphere at 37 °C. MWCNT were added to the culture medium to a final concentration of 5 μg/mL, following which the suspensions were either: (i) vortexed for 15 s, sonicated for 15 min, and vortexed again for 15 s to obtain dispersed (D) tubes, or (ii) vortexed without sonication to obtain the non-dispersed (ND) tube suspension. After exposure to the dispersed (D) and non-dispersed (ND) MWCNT for 48 hr, CRL-1490 cells were fixed and stained with the EdU and Hoechst dyes according to manufacturer's instructions included in the Click-iT EdU cell proliferation kit (Invitrogen, Carlsbad, CA, USA). Growth proliferation was assessed by calculating the percentage of cells in the culture that incorporates the fluorescent EdU into newly synthesized DNA. Please notice that because the EMEM is similar to the DMEM composition, there were no differences in the hydrophobicity index, suspension stability index, rate of agglomeration and dynamic light scattering results in the former medium (not shown).

Supplementary Material

Refer to Web version on PubMed Central for supplementary material.

Acknowledgments

References

1. Iijima S. Helical Microtubules of Graphitic Carbon. Nature. 1991; 354:56–58.

2. Lin Y, Taylor S, Li HP, Fernando KAS, Qu LW, Wang W, Gu LR, Zhou B, Sun YP. Advances Toward Bioapplications of Carbon Nanotubes. J Mater Chem. 2004; 14:527–541.

3. Baughman RH, Zakhidov AA, de Heer WA. Carbon Nanotubes--the Route toward Applications. Science. 2002; 297:787–792. [PubMed: 12161643]

4. Nel A, Xia T, Madler L, Li N. Toxic Potential of Materials at the Nanolevel. Science. 2006; 311:622–627. [PubMed: 16456071]

5. Muller J, Delos M, Panin N, Rabolli V, Huaux F, Lison D. Absence of Carcinogenic Response to Multiwall Carbon Nanotubes in a 2-Year Bioassay in the Peritoneal Cavity of the Rat. Toxicol Sci. 2009; 110:442–448. [PubMed: 19429663]

6. Muller J, Huaux F, Moreau N, Misson P, Heilier JF, Delos M, Arras M, Fonseca A, Nagy JB, Lison D. Respiratory Toxicity of Multi-wall Carbon Nanotubes. Toxicol Appl Pharmacol. 2005; 207:221–231. [PubMed: 16129115]

7. Shvedova AA, Kisin ER, Mercer R, Murray AR, Johnson VJ, Potapovich AI, Tyurina YY, Gorelik O, Arepalli S, Schwegler-Berry D, et al. Unusual Inflammatory and Fibrogenic Pulmonary Responses to Single-Walled Carbon Nanotubes in Mice. Am J Physiol-Lung Cell Mol Physiol. 2005; 289:L698–L708. [PubMed: 15951334]

8. Warheit DB, Laurence BR, Reed KL, Roach DH, Reynolds GAM, Webb TR. Comparative Pulmonary Toxicity Assessment of Single-Wall Carbon Nanotubes in Rats. Toxicol Sci. 2004; 77:117–125. [PubMed: 14514968]

9. Lam CW, James JT, McCluskey R, Hunter RL. Pulmonary Toxicity of Single-Wall Carbon Nanotubes in Mice 7 and 90 Days after Intratracheal Instillation. Toxicol Sci. 2004; 77:126–134. [PubMed: 14514958]

10. Chou CC, Hsiao HY, Hong QS, Chen CH, Peng YW, Chen HW, Yang PC. Single-Walled Carbon Nanotubes Can Induce Pulmonary Injury in Mouse Model. Nano Lett. 2008; 8:437–445. [PubMed: 18225938]

11. Meng H, Xia T, George S, Nel AE. A Predictive Toxicological Paradigm for the Safety Assessment of Nanomaterials. ACS Nano. 2009; 3:1620–1627. [PubMed: 21452863]

12. Mercer RR, Scabilloni J, Wang L, Kisin E, Murray AR, Schwegler-Berry D, Shvedova AA, Castranova V. Alteration of Deposition Pattern and Pulmonary Response as a Result of Improved Dispersion of Aspirated Single-Walled Carbon Nanotubes in a Mouse Model. Am J Physiol-Lung Cell Mol Physiol. 2008; 294:L87–L97. [PubMed: 18024722]

13. Girifalco LA, Hodak M, Lee RS. Carbon Nanotubes, Buckyballs, Ropes, and a Universal Graphitic Potential. Phys Rev B. 2000; 62:13104–13110.

14. Liu J, Casavant MJ, Cox M, Walters DA, Boul P, Lu W, Rimberg AJ, Smith KA, Colbert DT, Smalley RE. Controlled Deposition of Individual Single-Walled Carbon Nanotubes on Chemically Functionalized Templates. Chem Phys Lett. 1999; 303:125–129.

15. Ausman KD, Piner R, Lourie O, Ruoff RS, Korobov M. Organic Solvent Dispersions of Single-Walled Carbon Nanotubes: Toward Solutions of Pristine Nanotubes. J Phys Chem B. 2000; 104:8911–8915.

16. Kang S, Mauter MS, Elimelech M. Microbial Cytotoxicity of Carbon-Based Nanomaterials: Implications for River Water and Wastewater Effluent. Environ Sci Technol. 2009; 43:2648–2653. [PubMed: 19452930]

17. Hyung H, Kim JH. Natural Organic Matter (NOM) Adsorption to Multi-walled Carbon Nanotubes: Effect of NOM Characteristics and Water Quality Parameters. Environ Sci Technol. 2008; 42:4416–4421. [PubMed: 18605564]

18. Saleh NB, Pfefferle LD, Elimelech M. Aggregation Kinetics of Multiwalled Carbon Nanotubes in Aquatic Systems: Measurements and Environmental Implications. Environ Sci Technol. 2008; 42:7963–7969. [PubMed: 19031888]

19. Shvedova AA, Castranova V, Kisin ER, Schwegler-Berry D, Murray AR, Gandelsman VZ, Maynard A, Baron P. Exposure to Carbon Nanotube Material: Assessment of Nanotube Cytotoxicity Using Human Keratinocyte Cells. J Toxicol Environ Health-Part A. 2003; 66:1909–1926. [PubMed: 14514433]

20. Jia G, Wang HF, Yan L, Wang X, Pei RJ, Yan T, Zhao YL, Guo XB. Cytotoxicity of Carbon Nanomaterials: Single-Wall Nanotube, Multi-Wall Nanotube, and Fullerene. Environ Sci Technol. 2005; 39:1378–1383. [PubMed: 15787380]

21. Sager TM, Porter DW, Robinson VA, Lindsley WG, Schwegler-Berry DE, Castranova V. Improved Method to Disperse Nanoparticles for *In Vitro* and *In Vivo* Investigation of Toxicity. Nanotoxicology. 2007; 1:118–129.

22. Porter D, Sriram K, Wolfarth M, Jefferson A, Schwegler-Berry D, Andrew M, Castranova V. A biocompatible Medium for Nanoparticle Dispersion. Nanotoxicology. 2008; 2:144–154.

23. Elgrabli D, Abella-Gallart S, Aguerre-Chariol O, Robidel F, Rogerieux F, Boczkowski J, Lacroix G. Effect of BSA on Carbon Nanotube Dispersion for *In Vivo* and *In Vitro* Studies. Nanotoxicology. 2007; 1:266–278.

24. Vaisman L, Wagner HD, Marom G. The Role of Surfactants in Dispersion of Carbon Nanotubes. Adv Colloid Interfac. 2006; 128:37–46.

25. Rector DR, Bunker BC. Effect of Colloidal Aggregation on the Sedimentation and Rheological Properties of Tank Waste. PNL-10761. 1995:2.4–2.5.

26. Xia T, Kovochich M, Liong M, Zink JI, Nel AE. Cationic Polystyrene Nanosphere Toxicity Depends on Cell-specific Endocytic and Mitochondrial Injury Pathways. ACS Nano. 2008; 2:85–96. [PubMed: 19206551]

27. Xia T, Kovochich M, Liong M, Madler L, Gilbert B, Shi HB, Yeh JI, Zink JI, Nel AE. Comparison of the Mechanism of Toxicity of Zinc Oxide and Cerium Oxide Nanoparticles Based on Dissolution and Oxidative Stress Properties. ACS Nano. 2008; 2:2121–2134. [PubMed: 19206459]

28. Ji Z, Jin X, George S, Xia T, Meng H, Wang X, Suarez E, Zhang H, Hoek EM, Godwin H, et al. Dispersion and Stability Optimization of TiO(2) Nanoparticles in Cell Culture Media. Environ Sci Technol. 2010; 44:7309–7314. [PubMed: 20536146]

29. Chen RJ, Bangsaruntip S, Drouvalakis KA, Kam NWS, Shim M, Li YM, Kim W, Utz PJ, Dai HJ. Noncovalent Functionalization of Carbon Nanotubes for Highly Specific Electronic Biosensors. Proc Natl Acad Sci U S A. 2003; 100:4984–4989. [PubMed: 12697899]

30. Strano MS, Moore VC, Miller MK, Allen MJ, Haroz EH, Kittrell C, Hauge RH, Smalley RE. The Role of Surfactant Adsorption During Ultrasonication in the Dispersion of Single-Walled Carbon Nanotubes. J Nanosci Nanotechnol. 2003; 3:81–86. [PubMed: 12908233]

31. Wang LY, Mercer RR, Rojanasakul Y, Qiu AJ, Lu YJ, Scabilloni JF, Wu NQ, Castranova V. Direct Fibrogenic Effects of Dispersed Single-Walled Carbon Nanotubes on Human Lung Fibroblasts. J Toxicol Environ Health-Part A. 2010; 73:410–422. [PubMed: 20155582]

32. Wilhelm C, Billotey C, Roger J, Pons JN, Bacri JC, Gazeau F. Intracellular Uptake of Anionic Superparamagnetic Nanoparticles as a Function of Their Surface Coating. Biomaterials. 2003; 24:1001–1011. [PubMed: 12504522]

33. Kratz F. Albumin as a Drug Carrier: Design of Prodrugs, Drug Conjugates and Nanoparticles. J Contr Release. 2008; 132:171–183.

34. Kam NWS, Liu ZA, Dai HJ. Carbon Nanotubes as Intracellular Transporters for Proteins and DNA: An Investigation of the Uptake Mechanism and Pathway. Angew Chem Int Edit. 2006; 45:577–581.

35. Pantarotto D, Briand JP, Prato M, Bianco A. Translocation of Bioactive Peptides Across Cell Membranes by Carbon Nanotubes. Chem Commun. 2004; 1:16–17.

36. Wang YB, Iqbal Z, Mitra S. Microwave-induced Rapid Chemical Functionalization of Single-Walled Carbon Nanotubes. Carbon. 2005; 43:1015–1020.

37. Wang YB, Iqbal Z, Mitra S. Rapidly Functionalized, Water-dispersed Carbon Nanotubes at High Concentration. J Am Chem Soc. 2006; 128:95–99. [PubMed: 16390136]

38. Wang Y, Iqbal Z, Mitra S. Rapid, Low Temperature Microwave Synthesis of Novel Carbon Nanotube-Silicon Carbide Composite. Carbon. 2006; 44:2804–2808.

39. Chen YH, Mitra S. Fast Microwave-Assisted Purification, Functionalization and Dispersion of Multi-Walled Carbon Nanotubes. J Nanosci Nanotechnol. 2008; 8:5770–5775. [PubMed: 19198303]

40. Thess A, Lee R, Nikolaev P, Dai HJ, Petit P, Robert J, Xu CH, Lee YH, Kim SG, Rinzler AG, et al. Crystalline Ropes of Metallic Carbon Nanotubes. Science. 1996; 273:483–487. [PubMed: 8662534]

41. Oberdorster G, Maynard A, Donaldson K, Castranova V, Fitzpatrick J, Ausman K, Carter J, Karn B, Kreyling W, Lai D, et al. Principles for Characterizing the Potential Human Health Effects from Exposure to Nanomaterials: Elements of a Screening Strategy. Part Fibre Toxicol. 2005; 2:8. [PubMed: 16209704]

42. Deguchi S, Yamazaki T, Mukai S, Usami R, Horikoshi K. Stabilization of C-60 Nanoparticles by Protein Adsorption and Its Implications for Toxicity Studies. Chem Res Toxicol. 2007; 20:854–858. [PubMed: 17503852]

43. Chen W, Duan L, Zhu D. Adsorption of Polar and Nonpolar Organic Chemicals to Carbon Nanotubes. Environ Sci Technol. 2007; 41:8295–8300. [PubMed: 18200854]

44. George S, Kishen A. Effect of Tissue Fluids on Hydrophobicity and Adherence of Enterococcus Faecalis to Dentin. J Endod. 2007; 33:1421–1425. [PubMed: 18037050]

45. Worsley KA, Kalinina I, Bekyarova E, Haddon RC. Functionalization and Dissolution of Nitric Acid Treated Single-Walled Carbon Nanotubes. J Am Chem Soc. 2009; 131:18153–18158. [PubMed: 19919061]

46. Schudel M, Behrens SH, Holthoff H, Kretzschmar R, Borkovec M. Absolute Aggregation Rate Constants of Hematite Particles in Aqueous Suspensions: A Comparison of Two Different Surface Morphologies. J Colloid Interface Sci. 1997; 196:241–253. [PubMed: 9792750]

47. Chen KL, Elimelech M. Influence of Humic Acid on the Aggregation Kinetics of Fullerene (C-60) Nanoparticles in Monovalent and Divalent Electrolyte Solutions. J Colloid Interface Sci. 2007; 309:126–134. [PubMed: 17331529]

48. Chen KL, Mylon SE, Elimelech M. Aggregation Kinetics of Alginate-coated Hematite Nanoparticles in Monovalent and Divalent Electrolytes. Environ Sci Technol. 2006; 40:1516–1523. [PubMed: 16568765]
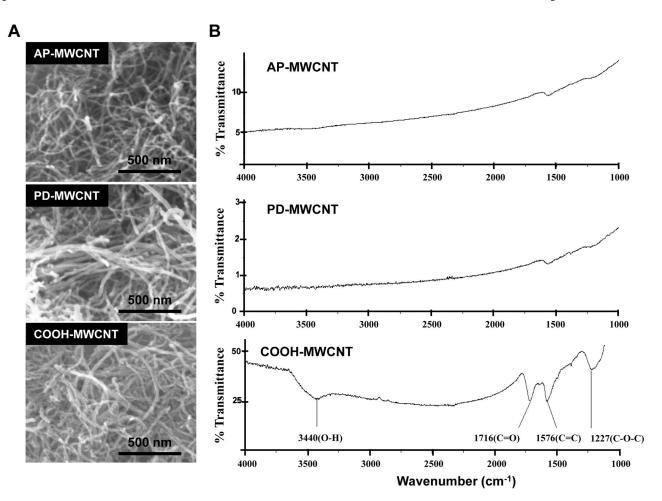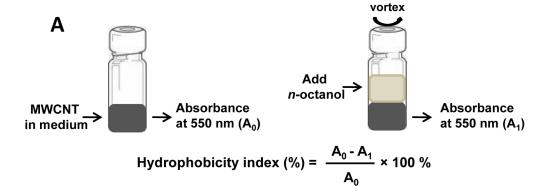
Figure 1.
Physicochemical characterization of the AP-MWCNT, PD-MWCNT and COOH-MWCNT.
A: Representative scanning electronic microscopy (SEM) images of AP-MWCNT, PD-MWCNT and COOH-MWCNT. Pictures were taken with a Genesis 4000 XMS SEM, (EDAX Inc., Mahwah, NJ, USA). Magnification is 200,000×. B: The Fourier Transform Infrared spectroscopy spectra done by a PerkinElmer Spectrum One instrument (Downers Grove, IL, USA) show the carboxyl functionalization of the COOH-MWCNT.
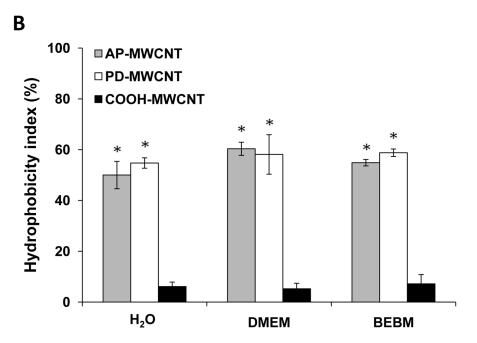
A

$$\text{Hydrophobicity index (\%)} = \frac{A_0 - A_1}{A_0} \times 100\ \%$$

B

Figure 2.
Determination of the hydrophobicity index of AP-, PD- and COOH-MWCNT in H_2O, DMEM and BEBM using partitioning in an *n*-octanol/aqueous interface. The hydrophobicity index of the tubes suspended in the aqueous phase at 50 μg/mL was calculated by the absorbance reading at 550 nm in H_2O, DMEM and BEBM (A_0) prior to and following (A_1) the addition of *n*-octanol as described in Materials and Methods. The same experiment was carried out at different CNT concentrations (up to 120 μg/mL), which yielded the same results and therefore incorporated into the biological experiments (*e.g.*, Fig. 6) with the same trend.
* $p < 0.05$, compare to the COOH-MWCNT.
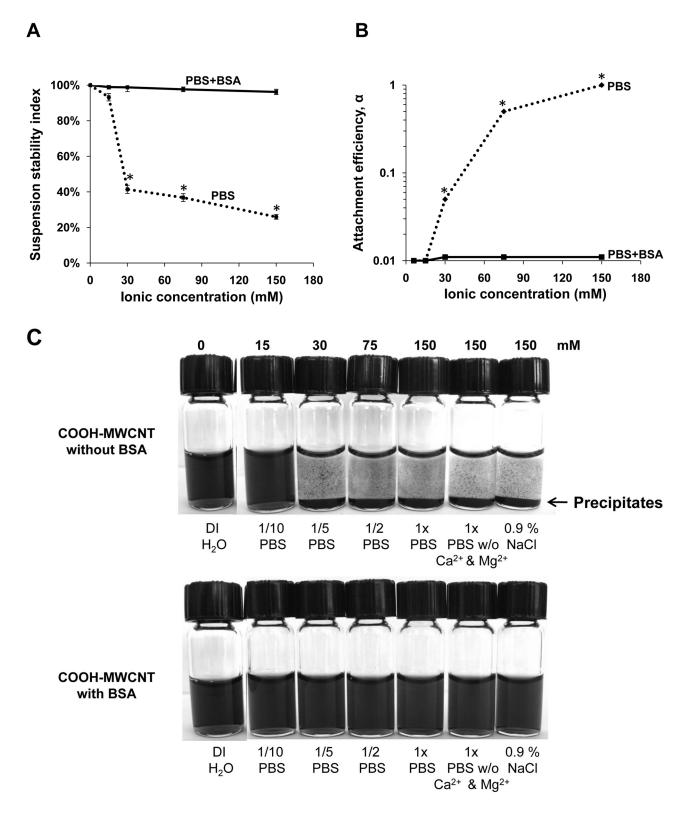
A

B

C

Figure 3.
Solution ionic strength affects the suspension stability index and the attachment efficiency of MWCNT in PBS and physiological media. A: The suspension stability index of the

COOH-MWCNT at 50 μg/mL was expressed as the % of the initial absorbance (λ=550 nm) for tubes incubated for 20 hr after sonication in PBS concentrations of 0 mM, 15 mM, 30 mM, 75 mM and 150mM. The absorbance measurements were carried out by a UV-vis spectrometer (SpectroMax M5e, Molecular Devices Corp., Sunnyvale, CA, USA) as described in Materials and Methods. B: The attachment efficiency (α) of COOH-MWCNT was calculated as a function of solution ionic strength. The attachment efficiency was calculated from the aggregation rate constant as described in Materials and Methods. C: The effect of BSA (0.6 mg/ml) on COOH-MWCNT agglomeration as determined by visual inspection of precipitate formation in the presence of incremental PBS concentrations or 0.9 % saline. The tubes were suspended by sonication as described in Materials and Methods in the absence or presence of 0.6 μg/mL BSA. The tubes were photographed 20 hr after sonication.
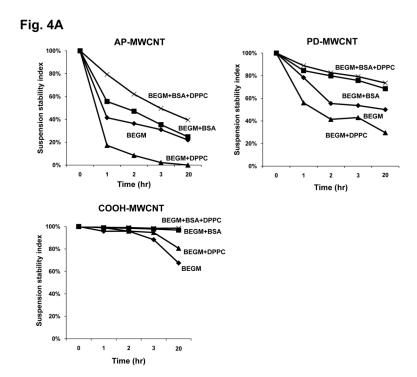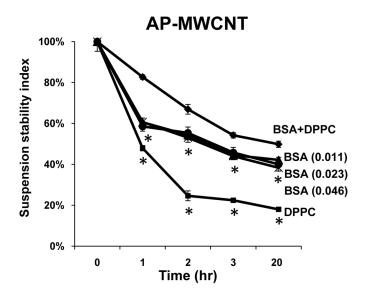
Fig. 4A

Fig. 4B

Figure 4.

Stability of AP-MWCNT, PD-MWCNT and COOH-MWCNT suspensions in BEGM in the absence or presence of dispersing agents [BSA (0.6 mg/mL) +/− DPPC (0.01 mg/mL)]. A: The suspension stability index of the MWCNT was determined as a function of time after suspension at 50 μg/mL in BEGM in the absence or presence of BSA, DPPC or BSA +DPPC. The suspension stability index was calculated as the % of initial MWCNT absorbance (t=0) at λ=550 nm for time periods of 1, 2, 3, and 20 hr. Absorbance was determined as described in Fig. 3. The stability of the AP-MWCNT suspension in BEGM +BSA+DPPC differed significantly ($p<0.05$) from the tubes being stabilized in BSA alone. B: The effect of BSA plus DPPC on AP-MWCNT stabilization is additive compared to equimolar BSA or DPPC concentrations. The suspension stability index of the tubes sonicated in 0.023 mM total dispersants (BSA = 0.009 mM, DPPC = 0.014 mM) is compared to 0.023 or 0.046 mM BSA as well as 0.023 mM DPPC. The addition of BSA plus DPPC significantly ($p<0.05$) enhanced AP-MWCNT stability compared to either BSA concentrations or an equimolar quantity of DPPC. BSA (0.011) = BSA at 0.011 mM; BSA (0.023) = BSA at 0.023 mM; BSA (0.046) = BSA at 0.046 mM in BEGM. Please notice that execution of the same experiment at different tube concentrations show BSA is capable of stabilizing the tubes in suspension over a wide dose range (see Fig. S5). * $p<0.05$ compared to the suspension stability index of AP-MWCNT in BEGM+BSA+DPPC.
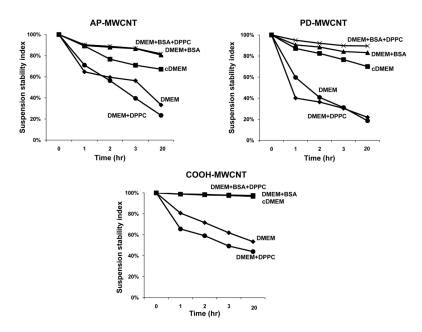
Figure 5.
Assessment of the suspension stability index of AP-MWCNT, PD-MWCNT and COOH-MWCNT in DMEM, with or without the addition of dispersing agents [BSA (0.6 mg/mL), DPPC (0.01 mg/mL) and 10 % FBS]. The suspension stability index of the MWCNT in DMEM was determined as described in Fig. 4A. The stability index is expressed as a % of the initial MWCNT absorbance (λ=550 nm) as described in Fig. 4.
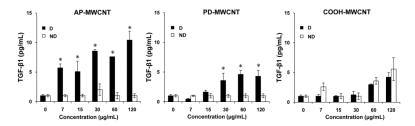
Figure 6.
Comparison of the effect of dispersed (D) with non-dispersed (ND) tubes on TGF-β1 release by BEAS-2B cells. Cells were treated with the indicated concentrations of the AP-, PD- and COOH-MWCNT that were either sonicated in the presence of BSA (0.6 mg/ml) + DPPC (0.01 mg/ml) for 24 hr or vortexed in the absence the dispersants (BSA and DPPC) or sonication. The supernatants were collected to measure the TGF-β1 levels by ELISA as described in Materials and Methods. Please notice that there was no TGF-β1 release in BEAS-2B cells in response to MWCNT exposures where tubes not dispersed in BSA was sonicated (data not shown). Thus, sonication by itself does not provide sufficient dispersion to influence biological response outcomes at cellular level.
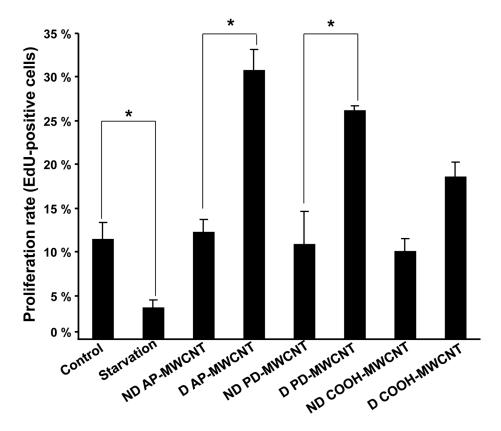* $p<0.05$, comparing non-dispersed (ND) to dispersed (D) tubes.

Figure 7.
Fibroblast proliferation rate in response to to MWCNT exposure. Fibroblast proliferation was assessed by an EdU proliferation assay. CRL-1490 cells (derived from pulmonary fibroblasts) were grown at a density of 5000 cells per well in 200 μL of EMEM supplemented with 10 % FBS. Dispersed (D) and non-dispersed (ND) MWCNTs were added to triplicate culture wells at a concentration of 5 μg/mL for 48 hr. A starvation condition (containing 1 % FBS) was included as a negative control. Cells were fixed and stained with the EdU and Hoechst dyes according to the manufacturer's instruction. Cells were viewed under an Axio Observer. D1 inverted microscope, (Carl Zeiss, Inc.). The number of proliferating cells incorporating the fluorescent dye EdU is quantitatively expressed as a percentage of the total cell population (Hoechst nuclear staining).

Table 1

Physicochemical Characterization of the MWCNTs[a]

	AP-MWCNT	PD-MWCNT	COOH-MWCNT
Outer Diameter (nm)	20–30	20–30	20–30
Inner Diameter (nm)	5–10	5–10	5–10
Length (μm)	10–30	10–30	10–30
Purity	around 94 %	> 95 %	> 95 %
Impurities (wt. %)	4.49 % Ni, 0.76 % Fe	1.80 % Ni, 0.08 % Fe	0.18 % S

[a]The outer, inner diameter and length distribution were measured using the SEM images of the MWCNT. The purity was measured by thermogravimetric analyses (TGA) using a Pyris 1 TGA (Perkin-Elmer Inc., Covina, CA, USA). The elemental composition was analyzed by energy dispersive X-ray spectroscopy (EDS, Oxford Instrument, Oxfordshire, UK). The experiment details are described in the Materials and Methods.

Table 2

Zeta potential and hydrodynamic size of the MWCNTs[a]

		AP-MWCNT	PD-MWCNT	COOH-MWCNT
Zeta potential (mV)	in H_2O (with BSA)	−14.50 (−28.61)	−8.73 (−31.76)	−50.30 (−29.35)
	in PBS (with BSA)	−14.08 (−10.94)	−13.12 (−11.31)	−13.08 (−10.13)
	in BEGM (with BSA)	−8.01 (−11.80)	−7.42 (−11.80)	−9.12 (−11.80)
	in DMEM (with BSA)	−12.85 (−7.22)	−13.20 (−9.64)	−13.45 (11.13)
Hydrodynamic size by DLS (nm)	in H_2O (with BSA)	324 (264)	858 (313)	134 (161)
	in PBS (with BSA)	713 (362)	718 (304)	1193 (243)
	in BEGM (with BSA)	779 (239)	650 (242)	1062 (310)
	in DMEM (with BSA)	1390 (248)	1492 (295)	1529 (230)

[a]The zeta potential measurement of the MWCNT suspension was performed using a ZetaSizer Nano-ZS instrument (Malvern Instruments, Worcestershire WR, UK). The MWCNT were suspended by sonication as described in Materials and Methods in the absence or presence of 0.6 µg/mL BSA. MWCNT hydrodynamic size in H_2O, PBS, BEGM and DMEM were measured using the dynamic light scattering (HT-DLS, Dynapro[TM] Plate Reader, Wyatt Technology, Santa Barbara, CA, USA). The experiment details are described in the Materials and Methods.